NATIONAL ADVISORY COMMITTEE FOR AERONAUTICS

WARTIME REPORT

ORIGINALLY ISSUED
September 1943 as
Advance [redacted] Report 3113

THEORY OF MECHANICAL OSCILLATIONS OF ROTORS WITH TWO HINGED BLADES

By Arnold M. Feingold

Langley Memorial Aeronautical Laboratory
Langley Field, Va.

NACA

WASHINGTON

NATIONAL ADVISORY COMMITTEE FOR AERONAUTICS

ADVANCE [redacted] REPORT

L-312

THEORY OF MECHANICAL OSCILLATIONS OF ROTORS WITH TWO HINGED BLADES

By Arnold M. Feingold

SUMMARY

The mechanical stability of a rotor having two vertically hinged blades mounted upon symmetrical supports, that is, of equal stiffness and mass in all directions, is investigated and reported herein. The frequency equation is derived and shows the existence, in general, of two ranges of rotational speeds at which instability occurs. The lower region of instability is bounded by two shaft-critical speeds. At rotor speeds within this region, self-excited divergence of the rotor takes place analogous to the instability exhibited by a rotating shaft that is elliptical in cross section. Within the second instability range, the rotor system undergoes self-excited oscillations. Charts are presented giving the boundary points of both instability regions for a large variety of values of the physical parameters. The effect of damping is also included in the analysis.

INTRODUCTION

In a recent report (reference 1), Coleman gives an analytical study of the mechanical stability of a rotor having three or more vertically hinged blades, mounted on flexible supports. It was shown that, in addition to the usual shaft-critical speeds, self-excited vibrations occurred over a range of rotational speeds. Experiments with rotary-wing aircraft have confirmed the soundness of the analysis.

The present paper is an investigation of the stability of the two-blade rotor mounted on symmetrical supports. As will be shown later, the results differ from those for a three-blade rotor. The reason for the different behavior

lies in the inherent asymmetry of a rotor with only two blades. Motion of the center of mass of the blades of a two-blade rotor with respect to the rotor hub, due to small hinge deflections of the blades, must be normal to the line of the blades. This restraint, which does not appear in a rotor of three or more blades, results in the rotor system having different dynamic properties along and normal to the line of the blades. Therefore, with supports that have equal stiffness and mass in all directions attached to a two-blade rotor, two principal vibration axes of the rotor hub can still be distinguished. No preferred vibration axes can be distinguished for a three-blade rotor mounted on symmetrical supports. This distinction shows up physically in the shape of the vibration modes. Whereas a three-blade rotor whirls in a circle, a two-blade rotor whirls in an ellipse, of which the principal axes are along and normal to the line of the rotor blades.

A two-blade rotor can be expected to show, in addition to some features of a three-blade rotor, some of the characteristics of a rotating shaft that is elliptical in cross section. Such a shaft, mounted on symmetrical bearings, is known to have two critical speeds, which correspond to each of the two principal stiffnesses. (See, for example, reference 2.) For all rotational speeds between the critical speeds, the shaft is unstable and diverges. It will be shown that an exactly similar phenomenon exists for a two-blade rotor. The existence of this region of instability for a two-blade rotor is predicted in reference 1, in which the formula for the shaft-critical speeds bounding this instability range is given. In addition to this region of instability, a second range of instability analogous to that exhibited by a three-blade rotor is also present.

Only the case of symmetrical supports is analyzed in the present report. In the case of asymmetric supports, the equations of motion are linear differential equations that are difficult to solve because the coefficients vary periodically with the time (Mathieu type). Similar equations are obtained in the problem of a rotating elliptical shaft mounted on asymmetric bearings. (See reference 2.)

SYMBOLS

a radial position of vertical hinge

b distance from vertical hinge to center of mass of blade

B	damping force per unit velocity of rotor–hub displacement
B_β	damping force per unit angular velocity of blade displacement about hinge
D	time–derivative operator (d/dt)
F	dissipation function
I	moment of inertia of blade about hinge $\left[m_b b^2 \left(1 + \frac{r^2}{b^2}\right)\right]$
K	spring constant of rotor–hub displacement
K_β	spring constant of blade self–centering spring
m	effective mass of pylon
m_b	effective mass of rotor blade
M	total effective mass of blades and pylon $(m + 2m_b)$
r	radius of gyration of blade about its center of mass
s	arbitrary parameter
t	time
T	kinetic energy
T_1, T_2	kinetic energies of rotor blades
T_s	kinetic energy of rotor hub
V	potential energy
x, y	displacements of rotor hub in rotating coordinate system
X_a, Y_a	rotating coordinate axes
X_f, Y_f	fixed coordinate axes
x_o, y_o	values of x and y when $t = 0$

x_1, y_1 displacement of first rotor blade in fixed coordinate system

x_2, y_2 displacement of second rotor blade in fixed coordinate system

β_1, β_2 angular displacements of blades about their hinges

$$\theta_0 = \frac{b(\beta_1 + \beta_2)}{2}$$

$$\theta_1 = \frac{b(\beta_1 - \beta_2)}{2}$$

θ_{1_0} = value of θ_1 when $t = 0$

$$\lambda = \frac{B}{M\omega_r}$$

$$\lambda_\beta = \frac{B_\beta}{I\omega_r}$$

$$\Lambda_1 = \frac{a}{b\left(1 + \frac{r^2}{b^2}\right)}$$

$$\Lambda_2 = \frac{K_\beta}{I\omega_r{}^2}$$

$$\Lambda_3 = \frac{m_b}{M\left(1 + \frac{r^2}{b^2}\right)}$$

ω angular velocity of rotor (the dimensionless ratio ω/ω_r is called ω in applications)

ω_a natural frequency of rotor system observed in rotating coordinate system (used in nondimensional form in applications)

ω_f natural frequency of rotor system in fixed coordinate system (nondimensional in applications)

ω_r reference frequency $(\sqrt{K/M})$

MATHEMATICAL ANALYSIS

Four degrees of freedom of the system are considered - horizontal deflection of the rotor hub in the x- and y-directions, and hinge deflections β_1 and β_2 of the blades in the horizontal plane of the rotor hub. The rotor is assumed to rotate at a constant velocity ω.

Deflection of the rotor hub may be due either to the bending of a flexible pylon or to a rocking of the rotor craft upon its landing gear. Ground-resonance vibrations usually involve landing-gear flexibility. The mathematical treatment is the same in both cases, but the values of several of the physical parameters will depend upon which mode is being investigated. Throughout this paper, the terms "rotor supports" and "pylon" will be used interchangeably to denote the nonrotating structure coupled with the rotor blades.

The mathematical treatment herein differs from that in reference 1, in which are used the complex notation and the notion of "whirling speeds," that is, directional frequencies, resulting from the use of complex numbers. Although the method of reference 1 is valuable for systems, such as the three-blade rotor on symmetrical supports, which have circular modes of vibration, it offers little advantage for the present problem, in which the rotor performs elliptical motion. Rectangular coordinates accordingly are used in the present paper and frequencies are used instead of whirling speeds. In comparing the results of the present paper with those of reference 1, care should be taken to distinguish between frequencies and whirling speeds. Whirling speeds have directional significance; whereas frequencies are essentially positive quantities and do not give any immediate information concerning the direction of whirl of the vibration.

The equations of motion are set up in a coordinate system rotating at the velocity ω. Let the deflection of the rotor hub be represented by x and y in rotating

coordinates. (See fig. 1 in which the intersection of the coordinate axes represents the undisturbed position of the rotor hub.) The disturbed positions of the two blades in fixed coordinates are

$$x_1 = (x + a + b\cos\beta_1)\cos\omega t - (y + b\sin\beta_1)\sin\omega t$$

$$y_1 = (y + b\sin\beta_1)\cos\omega t + (x + a + b\cos\beta_1)\sin\omega t$$

and

$$x_2 = (x - a - b\cos\beta_2)\cos\omega t - (y - b\sin\beta_2)\sin\omega t$$

$$y_2 = (y - b\sin\beta_2)\cos\omega t + (x - a - b\cos\beta_2)\sin\omega t$$

The kinetic energies of the two rotor blades are

$$T_1 = \frac{1}{2}m_b\left[\dot{x}_1^2 + \dot{y}_1^2 + r^2(\omega + \dot{\beta}_1)^2\right]$$

and

$$T_2 = \frac{1}{2}m_b\left[\dot{x}_2^2 + \dot{y}_2^2 + r^2(\omega + \dot{\beta}_2)^2\right]$$

The kinetic energy of the pylon is

$$T_s = \frac{1}{2}m\left[\dot{x}^2 + \dot{y}^2 + \omega^2(x^2 + y^2) - 2\omega(\dot{x}y - x\dot{y})\right]$$

Because only small displacements from the equilibrium position are considered, the trigonometric expressions containing β_1 and β_2 may be expanded as power series and only the terms that lead to quadratic terms in the energy expressions need be retained. Thus

$$\sin\beta_1 = \beta_1$$

$$\cos\beta_1 = 1 - \frac{\beta_1^2}{2}$$

and

$$\sin \beta_2 = \beta_2$$

$$\cos \beta_2 = 1 - \frac{\beta_2^2}{2}$$

New variables introduced to replace β_1 and β_2 are

$$\theta_0 = \frac{b}{2} (\beta_1 + \beta_2)$$

$$\theta_1 = \frac{b}{2} (\beta_1 - \beta_2)$$

where θ_1 represents the shift, due to hinge motion, of the center of mass of the two blades with respect to the rotor hub. The introduction of θ_0 and θ_1 results in a partial decoupling of the equations of motion.

The total kinetic energy of the system is

$$T = T_1 + T_2 + T_S$$

Only the quadratic terms will be retained in the kinetic-energy expression, because the terms of lower degree vanish in the Lagrange equations of motion. Then

$$T = \frac{1}{2}M \left[\dot{x}^2 + \dot{y}^2 + \omega^2 (x^2 + y^2) - 2\omega (\dot{x}y - x\dot{y})\right]$$

$$+ m_b \left[2\dot{y}\dot{\theta}_1 + 2\omega^2 y\theta_1 + 2\omega x\dot{\theta}_1 - 2\omega\dot{x}\theta_1 \right.$$

$$\left. + \left(1 + \frac{r^2}{b^2}\right)\left(\dot{\theta}_0^2 + \dot{\theta}_1^2\right) - \omega^2\frac{a}{b}\left(\theta_0^2 + \theta_1^2\right)\right]$$

The potential energy of the system is

$$V = \frac{1}{2} K \left(x^2 + y^2\right) + K_\beta \left(\beta_1^2 + \beta_2^2\right)$$

$$= \frac{1}{2} K \left(x^2 + y^2\right) + \frac{K_\beta}{b^2} \left(\theta_o^2 + \theta_1^2\right)$$

Two types of damping of the rotor system are assumed to exist: (1) damping in the rotor supports, which is proportional to velocity displacements of the rotor hub in a fixed coordinate system and (2) damping in the blade hinges. The dissipation function F then becomes

$$F = \frac{1}{2} B \left[\dot{x}^2 + \dot{y}^2 + \omega^2 \left(x^2 + y^2\right) - 2\omega \left(\dot{x}y - x\dot{y}\right)\right]$$

$$+ \frac{B_\beta}{b^2} \left(\dot{\theta}_o^2 + \dot{\theta}_1^2\right)$$

where B is the damping force per unit velocity of rotor-hub displacement and B_β is the damping force per unit velocity of a rotor-blade displacement about the blade hinge.

The Lagrange equations of motion are

$$\frac{d}{dt}\left(\frac{\partial T}{\partial \dot{x}}\right) - \frac{\partial T}{\partial x} + \frac{\partial V}{\partial x} + \frac{\partial F}{\partial \dot{x}} = 0$$

and similar expressions for y, θ_o, and θ_1. The equations of motion become

$$\left(D^2 + \omega^2 + \frac{B}{M}D + \frac{K}{M}\right) x - \frac{4m_b}{M}\omega\, D\theta_1 - \left(2\omega D + \frac{B}{M}\omega\right) y = 0 \qquad (1)$$

$$2\omega\, Dx + \left[\left(1 + \frac{r^2}{b^2}\right)D^2 + \frac{B_\beta}{m_b b^2}D + \frac{K_\beta}{m_b b^2} + \frac{a}{b}\omega^2\right] \theta_1 + \left(D^2 - \omega^2\right) y = 0 \qquad (2)$$

$$\left(2\omega D + \frac{B}{M}\omega\right) x + \frac{2m_b}{M}\left(D^2 - \omega^2\right) \theta_1 + \left(D^2 - \omega^2 + \frac{B}{M}D + \frac{K}{M}\right) y = 0 \qquad (3)$$

$$\left[\left(1 + \frac{r^2}{b^2}\right) D^2 + \omega^2 \frac{a}{b} + \frac{K_\beta}{m_b b^2}\right] \theta_o = 0 \qquad (4)$$

where the notation

$$D = \frac{d}{dt} \qquad D^2 = \frac{d^2}{dt^2}$$

is used.

Equation (4) can be solved independently of the others because it is an equation in only one variable θ_o. Equation (4), which also was obtained in the study of the three-blade rotor (reference 1), represents blade motion with the blades moving in phase, uncoupled with pylon motion. Motion in this mode is damped and does not lead to instability.

Assuming solutions of the form

$$\left.\begin{aligned} x &= x_o e^{i\omega_a t} \\ y &= y_o e^{i\omega_a t} \\ \theta_1 &= \theta_{1_o} e^{i\omega_a t} \end{aligned}\right\} \qquad (5)$$

and substituting these solutions in equations (1) to (3) gives the characteristic or frequency equation

$$\begin{vmatrix} -\omega_a^2 - \bar{\omega}^2 + i\lambda\omega_a + 1 & 4\Lambda_3\omega\omega_a & 2\omega\omega_a - i\lambda\omega \\ 2\omega\omega_a & -\omega_a^2 - i\lambda\beta\omega_a + \Lambda_2 + \Lambda_1\omega^2 & -\omega_a^2 - \omega^2 \\ 2\omega\omega_a - i\lambda\omega & -2\Lambda_3\left(\omega_a^2 + \omega^2\right) & -\omega_a^2 - \omega^2 + i\lambda\omega_a + 1 \end{vmatrix} = 0 \qquad (6)$$

where the nondimensional parameters

$$\Lambda_1 = \frac{a}{b\left(1 + \frac{r^2}{b^2}\right)}$$

$$\Lambda_2 = \frac{K_\beta}{I\omega_r^2}$$

$$\Lambda_3 = \frac{m_b}{M\left(1 + \frac{r^2}{b^2}\right)}$$

$$\lambda = \frac{B}{M\omega_r}$$

$$\lambda_\beta = \frac{B}{I\omega_r}$$

have been introduced, and the rotational velocity ω and the frequency ω_a have also been made nondimensional by using $\omega_r = \sqrt{K/M}$ as reference frequency.

The frequency ω_a generally is a complex number, of which the real part is the frequency of the vibration and the imaginary part determines the rate of damping of the vibration. If the imaginary part of ω_a is negative, the vibration increases in amplitude with time and the rotor is unstable.

DISCUSSION OF FREQUENCY EQUATION

Case of Zero Damping

If the damping parameters λ and λ_β are neglected, the frequency equation (6) may be expanded to

$$2\Lambda_3\left(\omega^2 + \omega_a{}^2 - 1\right)$$

$$+ \left[4\omega^2\omega_a{}^2 + \left(\omega^2 + \omega_a{}^2 - 1\right)^2\right]\left[-2\Lambda_3\left(\omega^2 + \omega_a{}^2 + 1\right)\right.$$

$$\left. + \omega_a{}^2 - \Lambda_2 - \Lambda_1\omega^2\right] = 0 \quad (7)$$

where ω_a is the natural frequency of the rotor system in a coordinate system rotating with the rotor. (Although equation (7) is a cubic equation in both ω^2 and $\omega_a{}^2$, rectangular hyperbolas of the form $\omega_a{}^2 = \omega^2 + s$, where s is an arbitrary parameter, intersect equation (7) at only two values of ω^2. For purposes of computation, therefore, equation (7) can be reduced to a quadratic equation in ω^2 by replacing $\omega_a{}^2$ with $\omega^2 + s$.)

The solutions for zero damping (equation (5)) represent motion of the pylon in an ellipse expressed relative to the rotating coordinate axes. In fixed coordinates, the pylon would move in an ellipse precessing at the velocity ω. This motion can be resolved into simultaneous circular motion at the two frequencies $|\omega + \omega_a|$ and $|\omega - \omega_a|$, in which the vertical lines indicate that the quantity inside is to be considered positive. If the pylon is subjected to a harmonic force in the fixed coordinate system of frequency ω_f, resonance will occur at each of the frequencies

$$\omega_f = |\omega \pm \omega_a|$$

The frequency ω_f will be referred to as the natural frequency of the rotor system in fixed coordinates.

The graph of the frequency equation (7) for a typical set of values of the parameters is given in figure 2 in rotating coordinates and in figure 3 in fixed coordinates. For zero coupling between the blades and rotor hub – that is, when Λ_3 equals zero – equation (7) factors into straight lines and a hyperbola, which are shown as long-dash lines in figures 2 and 3. The straight lines represent hub motion and the hyperbola represents blade motion. A small increase in Λ_3 results in a breaking away of the

curves at their intersections to form two self-excited regions. It is interesting to compare figure 3 with figure 4, which is the graph of the natural frequencies of a three-blade rotor having the same values of Λ_1, Λ_2, and Λ_3.

The shaft-critical speeds, or natural frequencies that would be in resonance with an unbalance in the rotor system, are found by putting $\omega_a = 0$ in equation (7). Figure 2 shows two such speeds, at points A and B (shown also in fig. 3), that bound a region in which ω_a is a pure imaginary number. If ω_a is a complex root of the characteristic equation, the complex conjugate of ω_a will also be a root and one of the two roots will have a negative imaginary part implying instability. The rotor system will thus be unstable for all rotational speeds between the two shaft-critical speeds. Because ω_a is a pure imaginary number in this region, the frequency of the resultant self-excited vibration is zero in a rotating coordinate system — similar to the shaft-critical speeds — and will appear as a self-excited divergence of the rotor.

The equation of the shaft-critical speeds is

$$\left[\left(1 - \omega^2\right)\left(\Lambda_2 + \Lambda_1\omega^2\right) - 2\Lambda_3\omega^4\right]\left(1 - \omega^2\right) = 0 \qquad (8)$$

The first factor gives the lower shaft-critical speed. The second factor, which depends on only the reference frequency, marks the end of the range of instability and is the second shaft-critical speed. Formula (8) and an experimental verification of it are given in reference 1. A convenient graph of equation (8) is given in figure 5. It will be noticed that it is impossible to remove the two shaft-critical speeds or the instability region between them by any possible change of the parameters Λ_1, Λ_2, or Λ_3; that is, without the introduction of damping, self-excited vibrations will always occur below the rotational speed ω_r.

Instability also occurs in a range of rotational speeds greater than ω_r. This range is shown in figures 2 and 3 as the region bounded by the points C and D and is similar in origin to the self-excited region exhibited by the three-blade rotor. In this region, the roots of the frequency equation are complex and self-excited vibrations will

take place. Unlike the three-blade rotor, however, the rotor hub will be seen from a stationary position to be simultaneously executing self-excited vibrations at two different frequencies. Physically, of course, the rotor is moving in an ellipse at the frequency ω_a while precessing at the velocity ω.

A chart showing the lower and upper limits of this instability region for a wide choice of values for the parameters Λ_1, Λ_2, and Λ_3 is given in figure 6. The chart is used by drawing a straight line that represents the function $(1 - 4\Lambda_3)\omega^2$ plotted against $\Lambda_1\omega^2 + \Lambda_2$. The intersections of this straight line with the proper Λ_3-curves give the desired values of ω. The short-dash line on the chart illustrates the method for the parameters of figure 2.

The position of the instability region is very sensitive to the value of Λ_3. (See fig. 7.) As Λ_3 increases, the region of instability occurs at greater rotational speeds and moves to infinity for $\Lambda_3 = 1/4$. For values of Λ_3 greater than $1/4$ - that is, when the total effective mass of the rotor blades is greater than the effective mass of the rotor supports - the self-excited region does not appear.

At certain rotational speeds, $\omega_f = 0$. At such speeds resonance may be excited by a steady force, constant in direction, acting on the pylon or blades - for example, gravity acting on a tilted rotor. The two-blade rotor has two such speeds, shown as points E and F in figures 2 and 3. The mathematical condition for such points is that $\omega_f = 0$ or $\omega_a^2 = \omega^2$ in equation (7). The equation giving the rotational speeds at which this condition may occur is

$$\left(\Lambda_1\omega^2 + \Lambda_2\right)\left(4\omega^2 - 1\right) - \omega^2\left[\omega^2\left(4 - 16\Lambda_3\right) - 1\right] = 0 \quad (9)$$

Equation (9) is plotted in figure 8, which is used similarly to figure 6.

Effect of Damping

The effect of damping will be determined in the same manner as for the three-blade rotor in reference 1. When

the damping parameters λ and λ_β are retained, equation (6) in expanded form can be separated into powers of ω_a having real and imaginary coefficients. The terms of equation (6) with real coefficients are

$$2\Lambda_3\left(\omega^2 + \omega_a{}^2 - 1\right) + \left[4\omega^2\omega_a{}^2 - \left(\omega^2 + \omega_a{}^2 - 1\right)^2\right]\left[-2\Lambda_3\left(\omega^2 + \omega_a{}^2 + 1\right) + \omega_a{}^2 - \Lambda_2 - \Lambda_1\omega^2\right] + \lambda^2\left(-\omega_a{}^2 + \Lambda_2 + \Lambda_1\omega^2\right)\left(\omega^2 - \omega_a{}^2\right) - 2\lambda\lambda_\beta\omega_a{}^2\left(\omega^2 - \omega_a{}^2 + 1\right) \quad (10)$$

The terms with imaginary coefficients are

$$i\lambda_\beta\omega_a\left\{2\frac{\lambda}{\lambda_\beta}\left[\left(\omega^2 - \omega_a{}^2 + 1\right)\left(\Lambda_1\omega^2 + \Lambda_2 - \omega_a{}^2\right) + \Lambda_3\left(3\omega^4 - 2\omega^2\omega_a{}^2 - \omega_a{}^4\right)\right] + \omega^4 + \omega_a{}^4 + 1 - 2\omega^2\omega_a{}^2 - 2\omega_a{}^2 - 2\omega^2 - \lambda^2\left(\omega_a{}^2 - \omega^2\right)\right\} \quad (11)$$

At a boundary between stability and instability, ω_a is real. Such points are the intersections of the equations formed by setting expressions (10) and (11) separately equal to zero and plotting them on the same coordinate axes. Figure 9 shows a calculated case of damping. The imaginary equation is plotted for several values of the ratio of the damping parameters λ/λ_β, with λ^2 assumed to be negligible. It is seen that, for large values of λ/λ_β, the boundaries of the higher range of instability are not far different from the boundaries found by neglecting damping. Small values of λ/λ_β — that is, when most of the damping is concentrated in the blade hinges — lead to a beginning of the instability at lower rotational speeds.

For small amounts of damping, the plot of the real equation is practically the same as when damping is neglected. By introducing sufficient damping, however, the higher instability region may be eliminated. (See fig. 10.) The two shaft-critical speeds and the instability region between them can also be removed by putting enough damping into the rotor supports, although a large amount of damping is required.

Brief Description of Vibration Modes

If damping is neglected, the shape of the free vibration modes can be found from the equations of motion (1) to (4) and the form of the solution, equation (5). The rotor hub generally moves in an elliptical path in rotating coordinates although, at certain speeds, the motion may become circular or linear. At zero rotational speed, two of the three modes involve hub motion normal to the line of the blades, with concomitant blade motion. In the third mode, the blades do not move about their hinges and the rotor hub moves in a straight line parallel to the line of the blades at a frequency equal to ω_r.

At the first shaft-critical speed, the rotor hub diverges in a direction normal to the line of the blades; whereas, at the second shaft-critical speed, the hub diverges parallel to the blades.

The forced responses of the system to a vibrator attached to the pylon can also easily be determined and show that those responses lying closest to the lines $\omega_f^2 = 1$ are the strongest. When the coupling parameter Λ_3 is zero, no response occurs along the lines $\omega_f = |2\omega \pm 1|$. This last conclusion is, of course, necessary if the theory is to give the correct results for the degenerate case of massless rotor blades.

CONCLUSIONS

The mechanical stability of a rotor having two vertically hinged blades mounted upon symmetrical supports has been investigated and reported herein. This investigation indicated that the main features of such a rotor system may be summarized as follows:

1. The vibration modes are generally elliptical, as opposed to circular for the three-blade rotor. The ellipse precesses at a speed ω as observed from a fixed position; the result is six resonant or natural frequencies in a fixed coordinate system for a given rotor speed as against four natural frequencies for the three-blade rotor.

2. The asymmetry of the two-blade-rotor system gives rise to a range of rotor speeds in which self-excited divergence of the rotor occurs. This instability region is bounded by two shaft-critical speeds. A three-blade rotor, in contrast, has only one shaft-critical speed with no associated instability region.

3. The two-blade rotor has a second region of rotational speeds at which self-excited vibrations occur.

Langley Memorial Aeronautical Laboratory,
National Advisory Committee for Aeronautics,
Langley Field, Va.

REFERENCES

1. Coleman, Robert P.: Theory of Self-Excited Mechanical Oscillations of Hinged Rotor Blades. NACA ARR No.3G29, 1943.

2. Foote, W. R., Poritsky, H., and Slade, J. J., Jr.: Critical Speeds of a Rotor with Unequal Shaft Flexibilities, Mounted in Bearings of Unequal Flexibility - I. Jour. Appl. Mech., vol. 10, no. 2, June 1943, pp. A-77 - A-84.

L-312

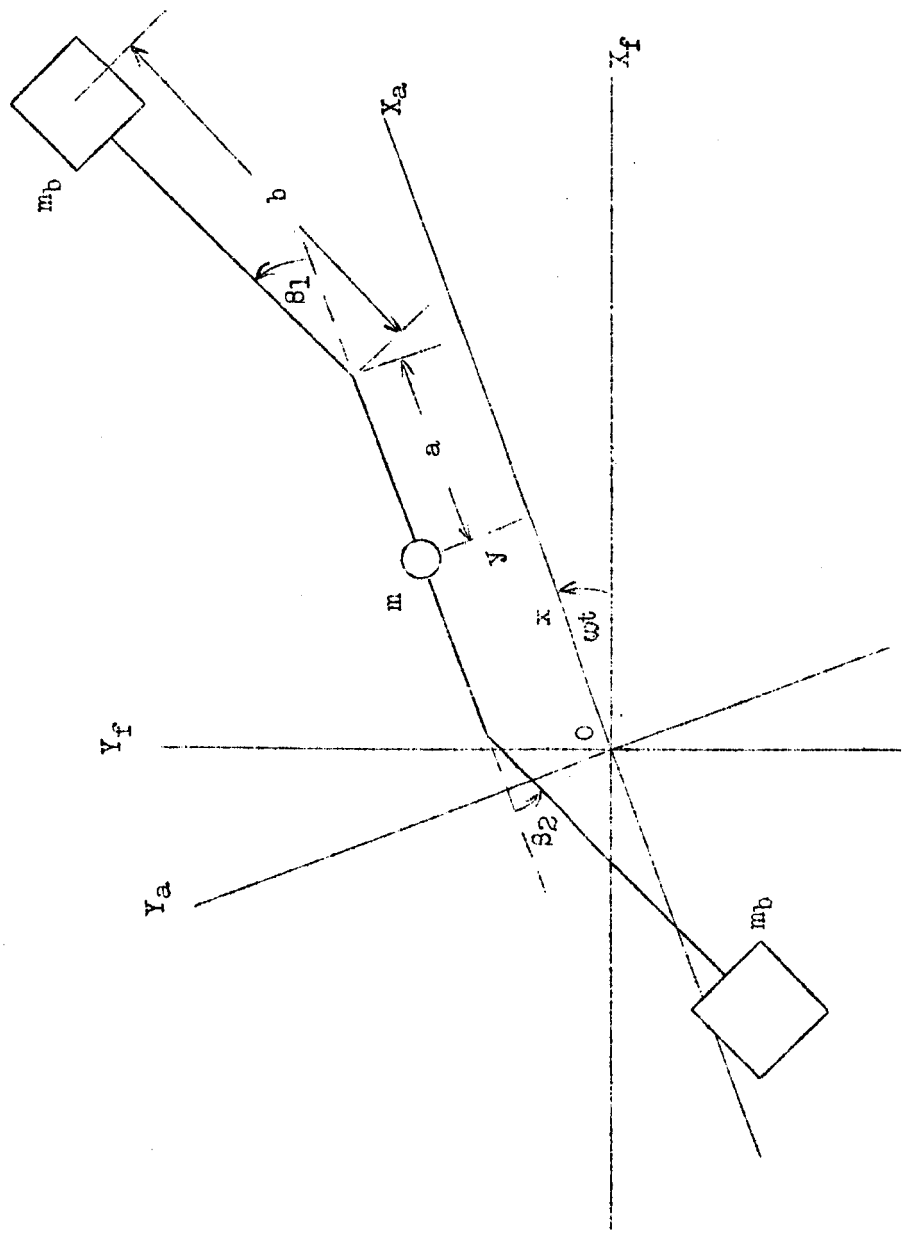

Figure 1.- Simplified mechanical system representing rotor.

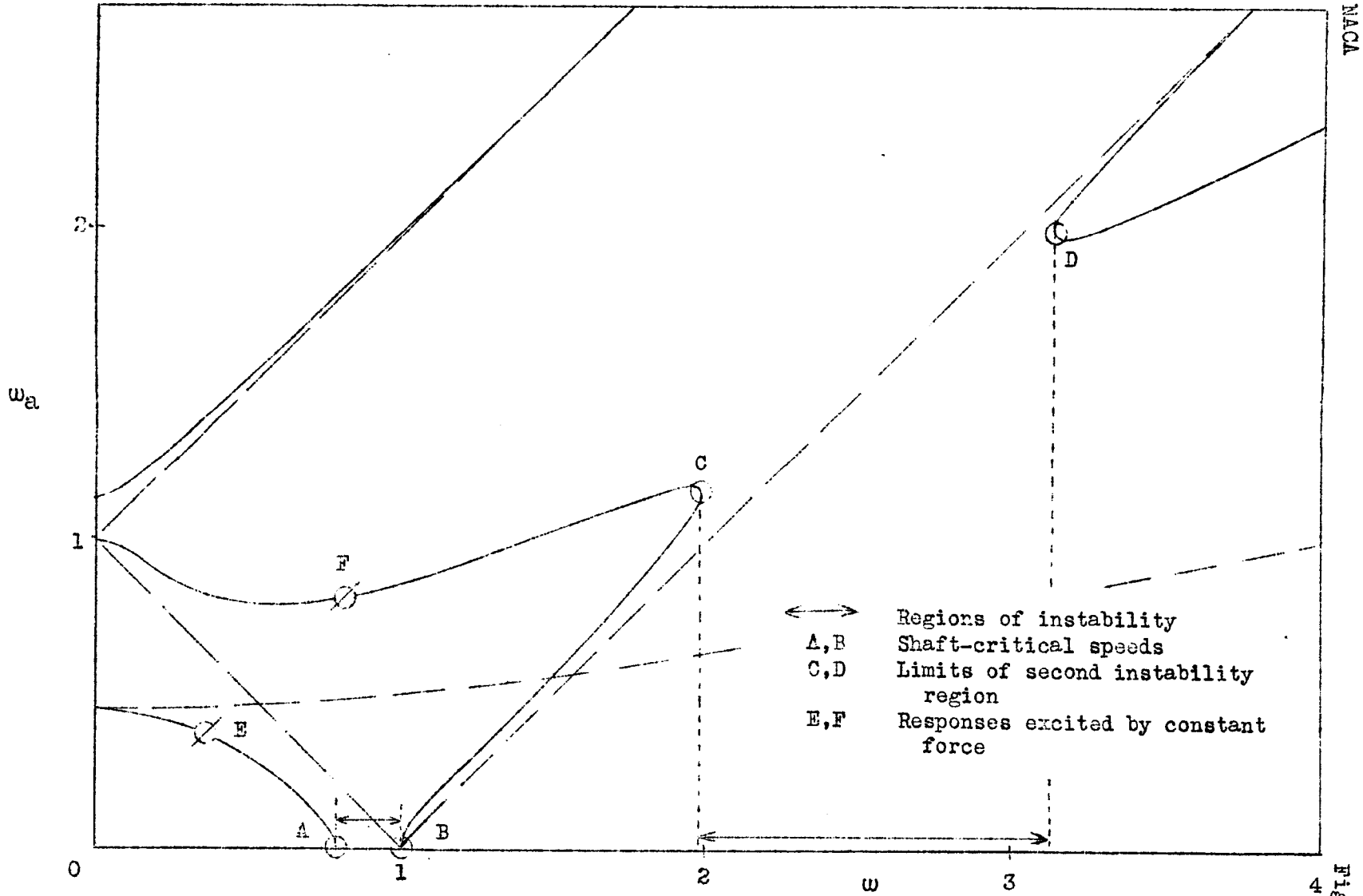

Figure 2.- Natural frequencies of a two-blade rotor in rotating coordinates for case of $\Lambda_1 = 0.05$, $\Lambda_2 = 0.20$, $\Lambda_3 = 0.10$.

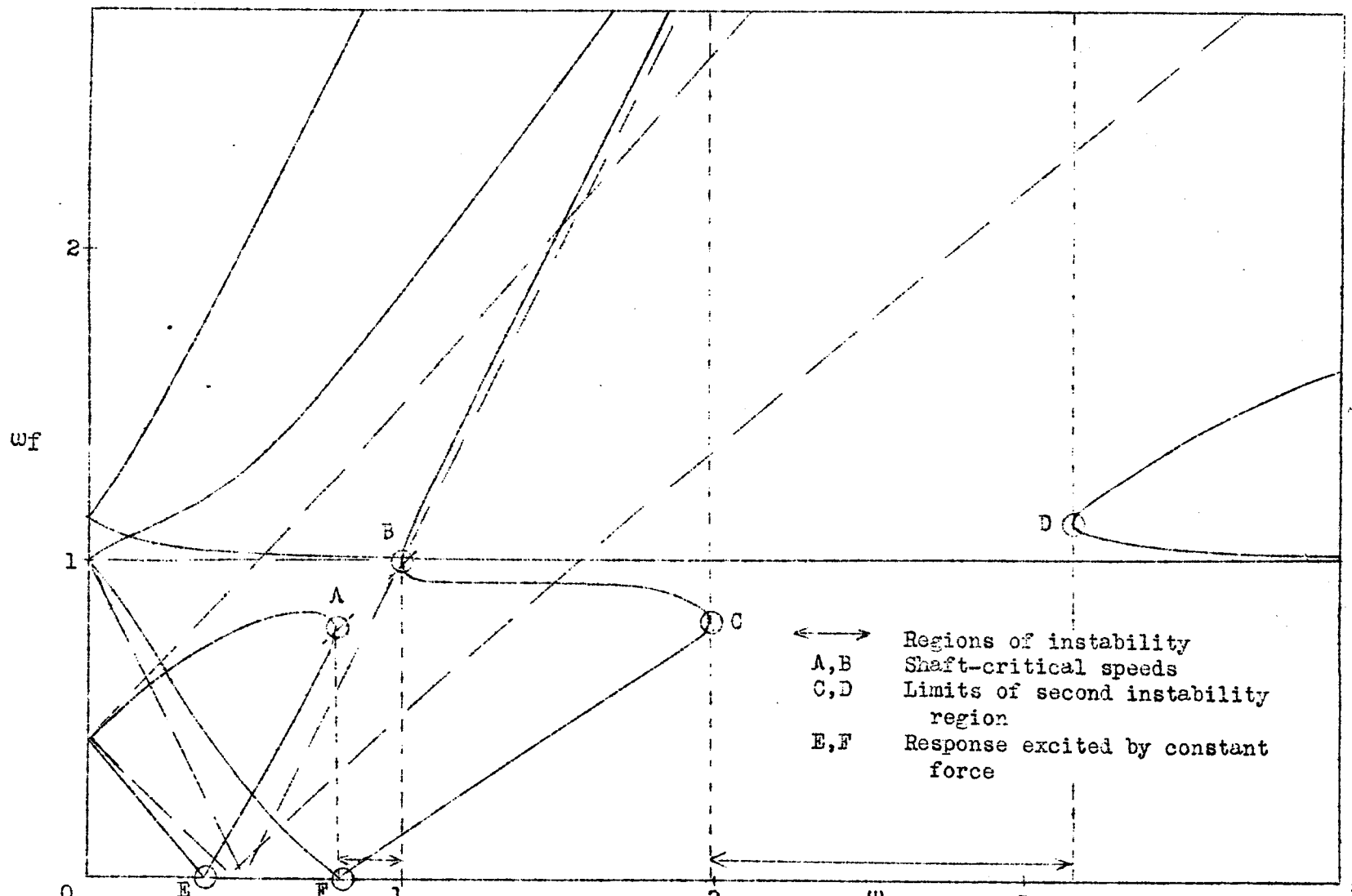

Figure 3.- Natural frequencies of a two-blade rotor in fixed coordinates for case of $\Lambda_1 = 0.05$, $\Lambda_2 = 0.20$, $\Lambda_3 = 0.10$.

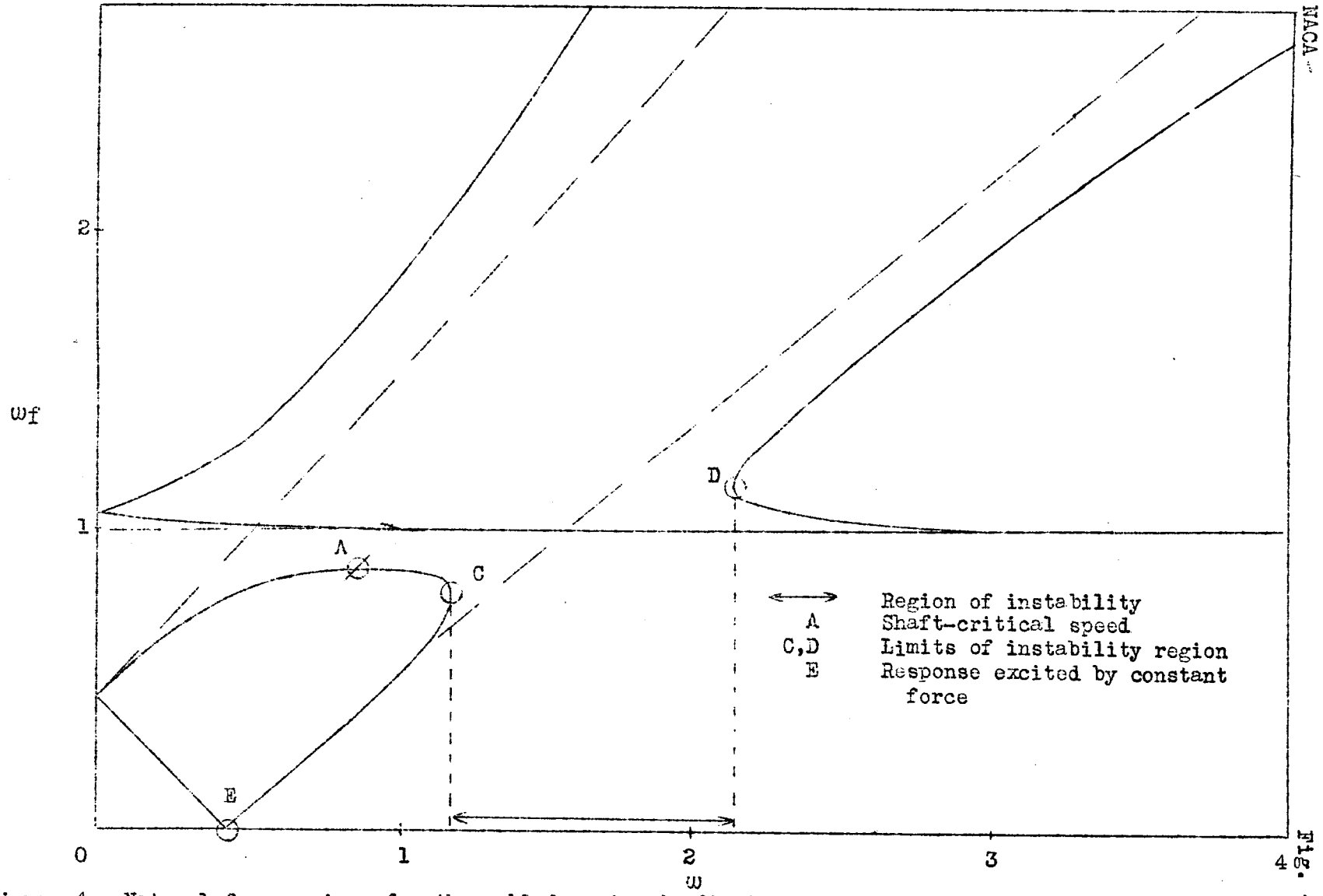

Figure 4.- Natural frequencies of a three-blade rotor in fixed coordinates for case of $\Lambda_1 = 0.05$, $\Lambda_2 = 0.20$, $\Lambda_3 = 0.10$.

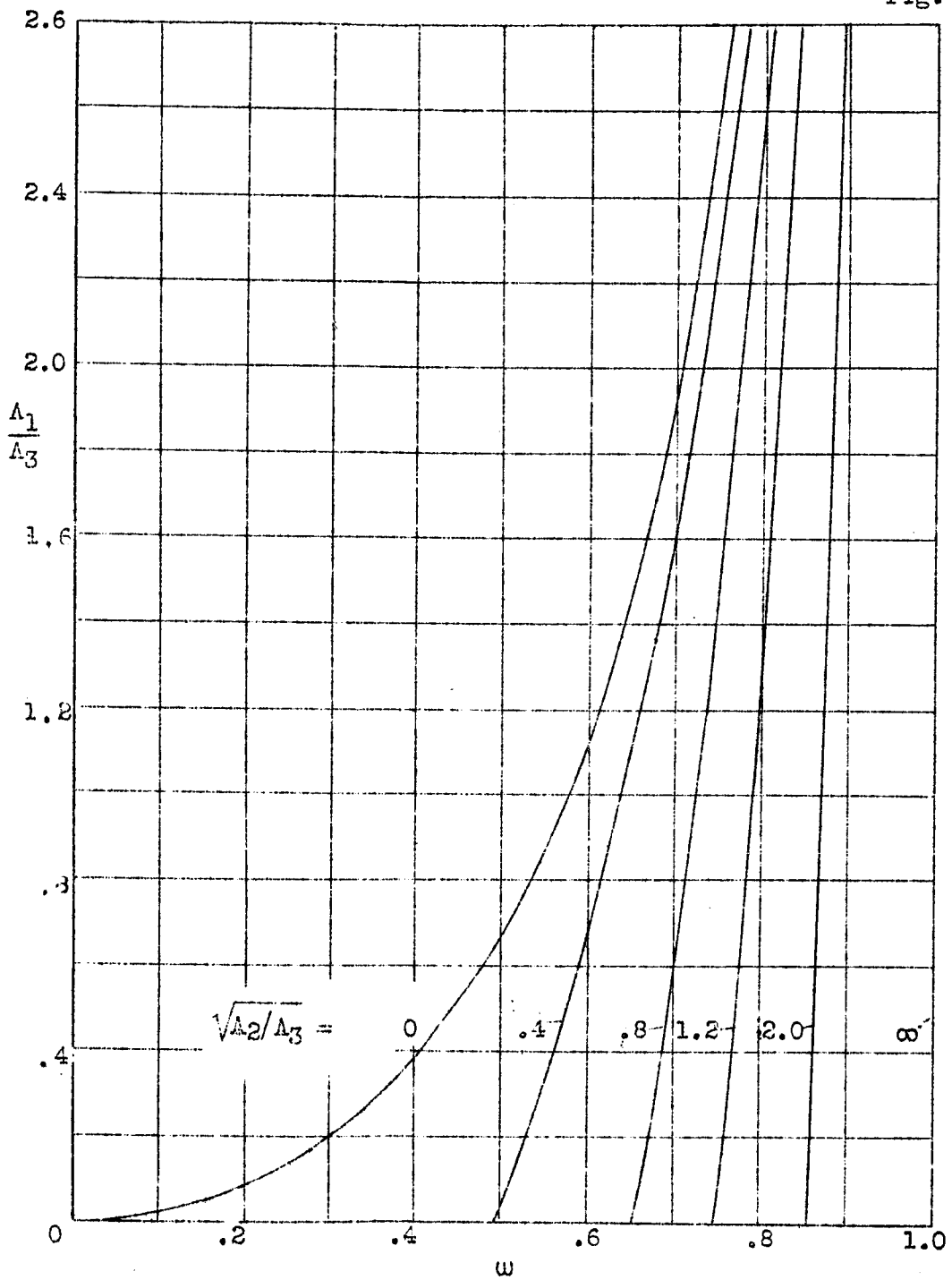

Figure 5.- Shaft-critical speeds.

L-312

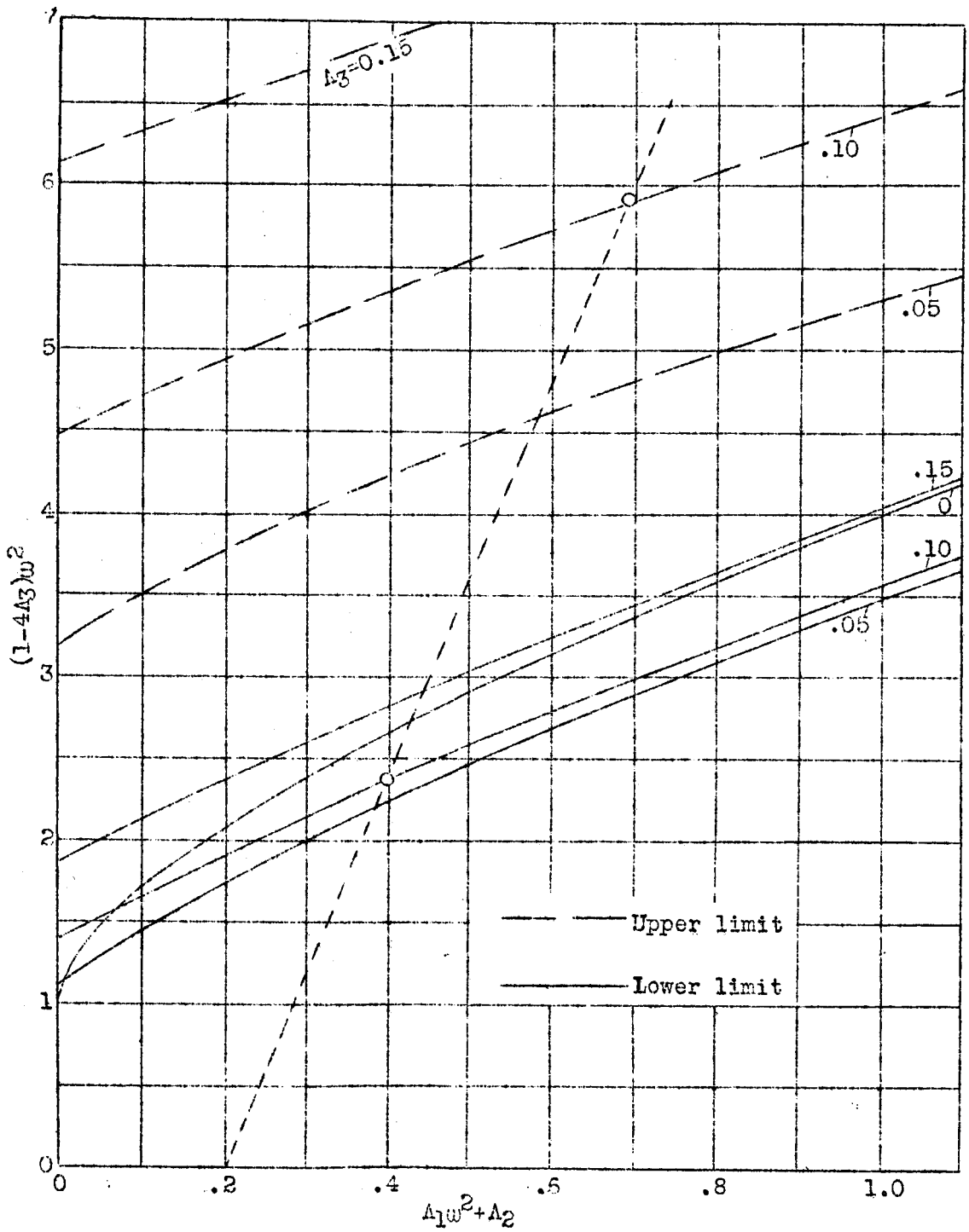

Figure 6.- Stability chart for second instability region.

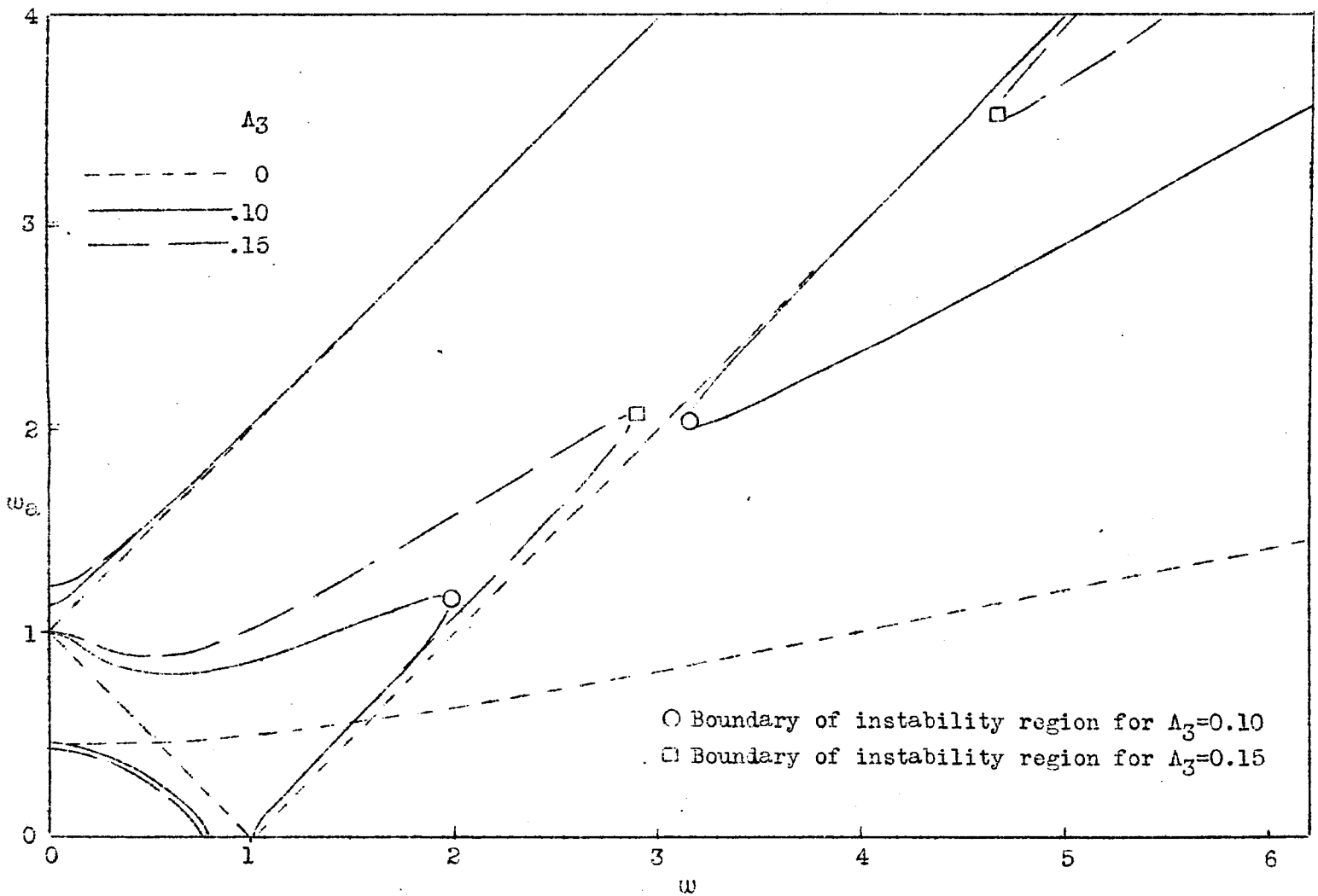

Figure 7.- Effect of coupling parameter Λ_3 for case of Λ_1=0.05, Λ_2=0.20.

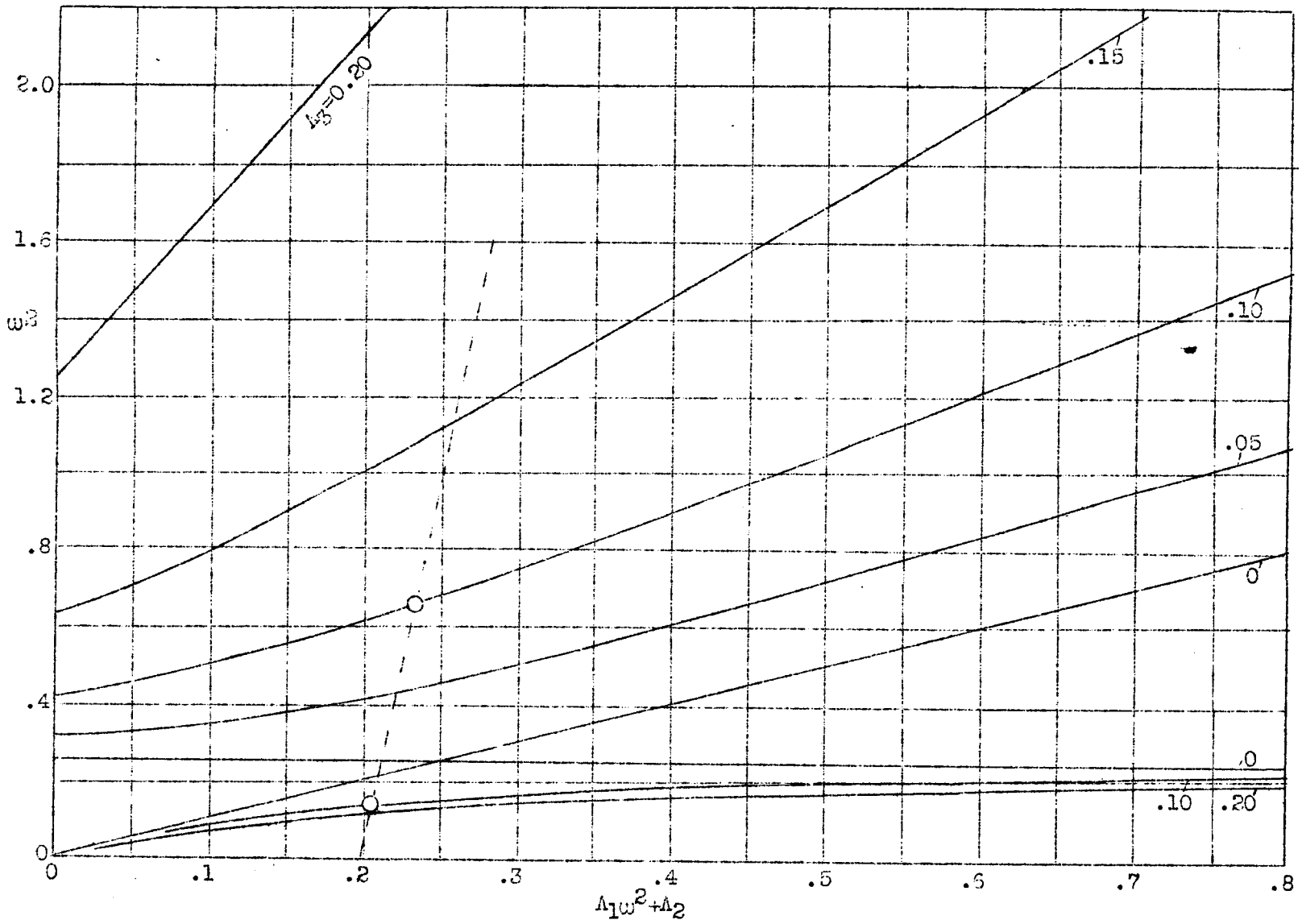

Figure 8.- Rotational speeds at which vibration could be excited by steady force.

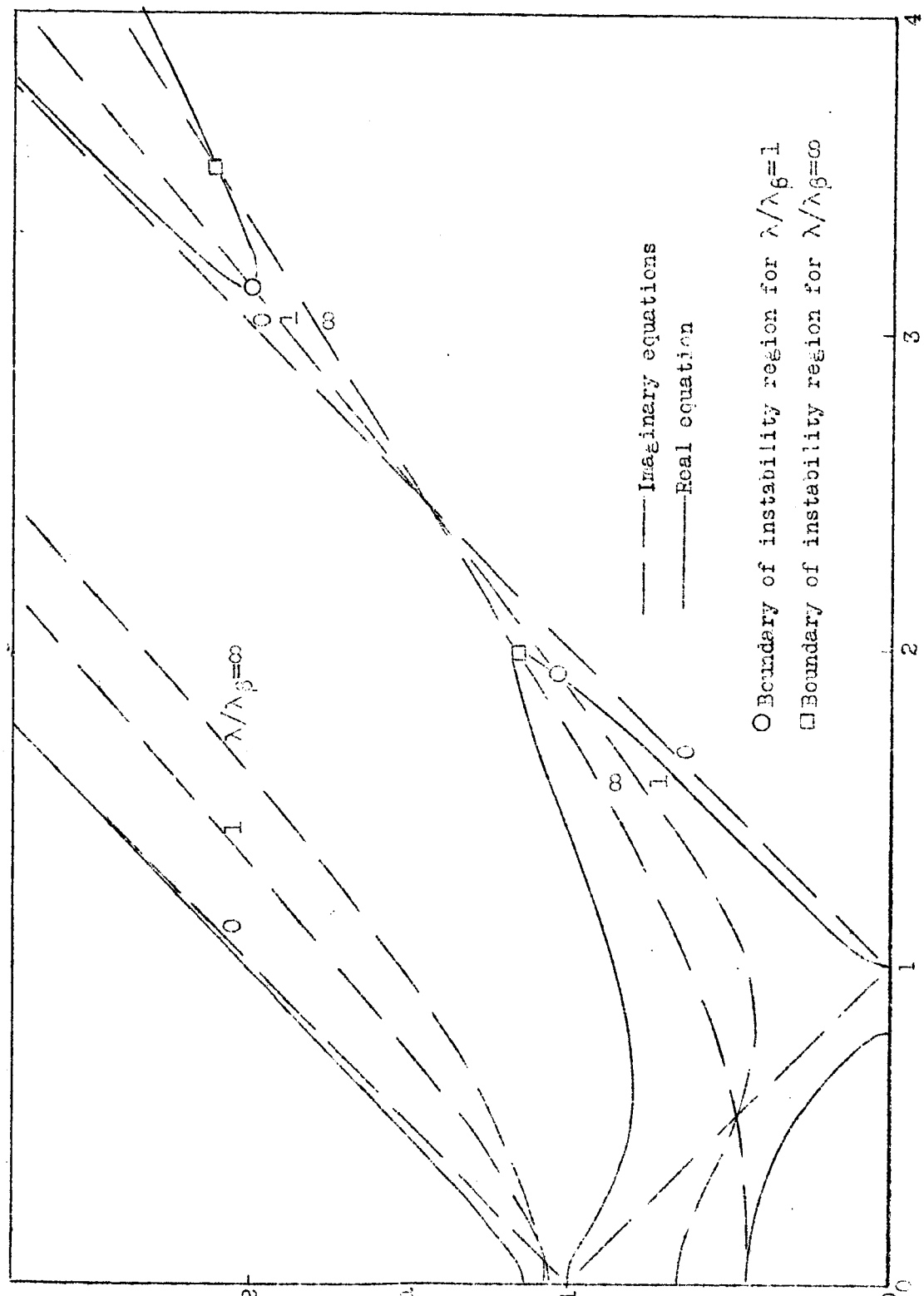

Figure 9.- Plot of real and imaginary equations for case of A_1=0.05, A_2=0.20, A_3=0.10, $\lambda\lambda_\beta \approx 0$.

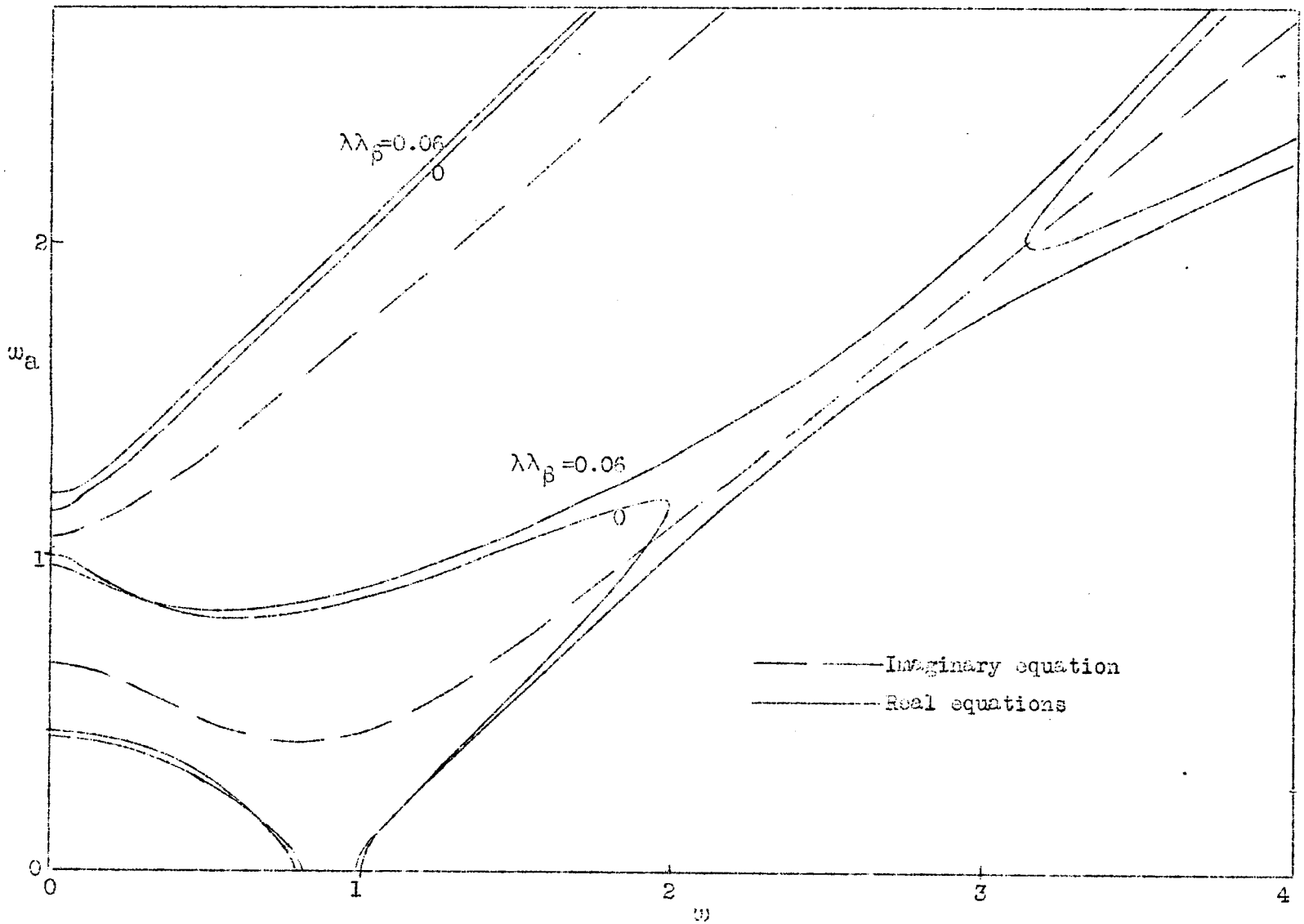

Figure 10.- Plot of real and imaginary equations for case of A_1=0.05, A_2=0.20, A_3=0.10, $\lambda=\lambda_\beta$.